

Constraints on the circumstellar dust around KIC 8462852

M.A. Thompson^{1*}, P. Scicluna², F. Kemper², J.E. Geach¹, M.M. Dunham³,
O. Morata², S. Ertel⁴, P.T.P. Ho^{2,5}, J. Dempsey⁵, I. Coulson⁵, G. Petitpas³,
L.E. Kristensen³

¹Centre for Astrophysics Research, School of Physics Astronomy & Mathematics, University of Hertfordshire, College Lane, Hatfield, Herts, AL10 9AB, UK

²Academia Sinica Institute of Astronomy and Astrophysics, P.O. Box 23-141, Taipei 10617, Taiwan

³Harvard-Smithsonian Center for Astrophysics, 60 Garden Street, Cambridge, MA 02138, USA

⁴European Southern Observatory, Alonso de Cordova 3107, Vitacura, Casilla 19001, Santiago, Chile

⁵East Asian Observatory, 660 N. Aohoku Place, University Park, Hilo, Hawaii 96720, USA

ABSTRACT

We present millimetre (SMA) and sub-millimetre (SCUBA-2) continuum observations of the peculiar star KIC 8462852 which displayed several deep and aperiodic dips in brightness during the *Kepler* mission. Our observations are approximately confusion-limited at 850 μm and are the deepest millimetre and sub-millimetre photometry of the star that has yet been carried out. No significant emission is detected towards KIC 8462852. We determine upper limits for dust between a few $10^{-6} M_{\oplus}$ and $10^{-3} M_{\oplus}$ for regions identified as the most likely to host occluding dust clumps and a total overall dust budget of $<7.7 M_{\oplus}$ within a radius of 200 AU. Such low limits for the inner system make the catastrophic planetary disruption hypothesis unlikely. Integrating over the *Kepler* lightcurve we determine that at least $10^{-9} M_{\oplus}$ of dust is required to cause the observed Q16 dip. This is consistent with the currently most favoured cometary breakup hypothesis, but nevertheless implies the complete breakup of ~ 30 Comet 1/P Halley type objects. Finally, in the wide SCUBA-2 field-of-view we identify another candidate debris disc system that is potentially the largest yet discovered.

Key words: stars: individual (KIC 8462852) – stars: peculiar – stars: circumstellar matter – submillimetre: stars – submillimetre: galaxies

1 INTRODUCTION

KIC 8462852 is one of the most peculiar stars discovered in the *Kepler* mission, exhibiting deep and aperiodic dips in its lightcurve that are so far unexplained (Boyajian et al. 2015, hereafter B15). KIC 8462852 (also known as TYC 3162-665-1 and 2MASS J20061546+4427248) is a main sequence F3 star with a possible wide M dwarf companion (B15, Lisse, Sitko & Marengo 2015). Over the period of the *Kepler* survey KIC 8462852 has a relatively constant brightness but during several periods the star underwent short-duration dips in brightness, including two events at a decrement of 15% and 22%. The lightcurves of these decreases, their durations and aperiodicity are not consistent with an origin of planetary transits.

B15 outline several possibilities for the decreases in brightness of KIC 8462852: instrumental effects; intrinsic stellar variability; catastrophic collisions of asteroids or plan-

etary bodies; dust enshrouded planetesimals, or a family of disrupted comets. B15 examine these possibilities in detail and are able to rule out instrumental effects and several classes of intrinsically variable stars, but find that no single hypothesis fits all the known facts. The disrupted cometary family hypothesis explains the lack of periodicity in the dips in brightness (due to eccentric orbits), but requires alternative “forward-tail” comet geometries to explain some of the lightcurves. B15 conducted a search for similar objects in the *Kepler* database and did not find any. They conclude that KIC 8462852 is almost certainly a unique phenomenon within the *Kepler* database.

Wright et al. (2015) have since put forward an alternative explanation that the dips in brightness may be caused by artificial structures orbiting the star. This suggestion is motivated by the original concept of the Dyson sphere (described in Dyson 1960, although strictly first conceived by Stapledon 1937) in which a space-dwelling civilisation may tap a substantial fraction of the energy of their host star by constructing large starlight collectors in orbit around the

* E-mail: m.a.thompson@herts.ac.uk

star. Such orbiting collectors may cause transits potentially observable by *Kepler* (Arnold 2005; Forgan 2013). Unsurprisingly this has provoked much speculation within the popular press on the existence of “alien megastructures” around the star. A targeted SETI search for persistent microwave signals from the vicinity of KIC 8462852 has so far proved negative (Harp et al. 2015).

Marengo, Hulsebus & Willis (2015, hereafter MHW15) recently presented warm *Spitzer* photometry of the star obtained during the SpiKeS *Spitzer Kepler* Survey. The *Spitzer* photometry at 3.6 and 4.5 μm is a factor of a few deeper than the *WISE* W1 and W2 measurements and was carried out 2 years after the dimming events observed by *Kepler*. The lack of significant excess in these wavebands leads these authors to conclude that the disrupted comet hypothesis of B15 is the preferred explanation. Lisse, Sitko & Marengo (2015) find no infrared excess in a 0.8–4.2 μm spectrum of the star and reach similar conclusions. However, one of the difficulties in understanding the nature of KIC 8462852 and the existence of any circumstellar dust is the paucity of observations of the star, particularly at longer wavelengths. No sensitive photometry of the star exists at wavelengths longer than 22 μm and thus no constraint exists upon the amount of cold dust that may be present in the outer regions of the system. Emission from cold dust would peak at longer wavelengths and be undetectable by the existing mid-infrared measurements.

In this Letter we present millimetre (mm) and sub-millimetre (sub-mm) wavelength observations of KIC 8462852 carried out with the Submillimeter Array and the SCUBA-2 camera on the James Clerk Maxwell Telescope. Our observations are the deepest existing mm and sub-mm photometry of this peculiar star and allow us to place sensitive constraints on the total amount of cold dust present in the system. In Section 2 we describe our observations and present a catalogue of detected 850 μm sources. In Section 3 we determine upper limits to the amount of dust present in the KIC 8462852 system and discuss these limits in relation to the hypotheses presented by B15. We discuss the nature of a candidate edge-on disc discovered in the wide SCUBA-2 FOV in Sect. 4 which is potentially the largest debris disc yet discovered. Finally we summarise our conclusions in Section 5.

2 OBSERVATIONS & RESULTS

2.1 SCUBA-2 Observations

We observed KIC 8462852 using the SCUBA-2 camera (Holland et al. 2013) mounted on the James Clerk Maxwell Telescope (JCMT) between October 26–29th 2015. We performed our observations using the “daisy” mapping mode, which is optimised for mapping objects smaller than the instantaneous FOV (Holland et al. 2013) and results in a map of $\sim 13'$ diameter. Approximately 6 hours of on-source observations were obtained. Atmospheric conditions were relatively dry during our observations, with a 225 GHz zenith opacity ranging between 0.06 and 0.1. The pointing accuracy of the telescope was checked on an hourly basis and found to be accurate to within $3''$. We regularly observed the calibrator CRL 2688 and estimate an absolute flux calibration of

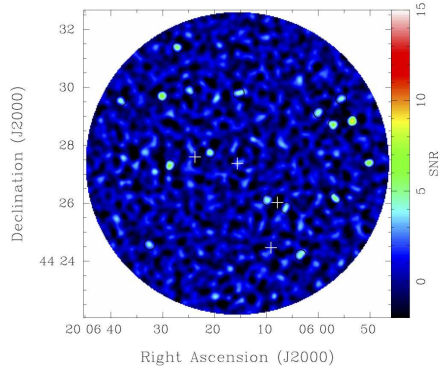


Figure 1. SCUBA-2 850 μm signal to noise map of the region surrounding KIC 8462852. Sources detected in the image at greater than 4σ confidence are indicated by circles and stars from the Tycho-2 catalogue are shown as crosses. KIC 8462852 is located at the centre of the image.

10% (Dempsey et al. 2013). We reduced the data with the Dynamic Iterative Map-Maker (Chapin et al. 2013) which is part of the *Starlink* SMURF package (Jenness et al. 2013). Given the likely compact nature of the expected emission we filtered the data at a scale of $150''$ in the map-making process to reduce the amount of low-frequency noise. A final beam matched filter was also applied to the map to enhance the sensitivity to point sources (Chapin et al. 2013). The resulting 450 and 850 μm maps have sensitivities of 10.7 and 0.85 mJy respectively in a central region of $5'$ diameter. A signal to noise map of the 850 μm data is shown in Fig. 1.

2.2 Submillimeter Array Observations

One track of observations of KIC 8462852 were obtained with the Submillimeter Array (SMA; Ho, Moran & Lo 2004) on the 10th November 2015 in the subcompact configuration with eight antennas, providing projected baselines ranging from 7 – 72 m. The observations were obtained with the 345 GHz receiver at a central frequency of 273 GHz (1.1 mm), with a total bandwidth of 11 GHz. The zenith opacity at 225 GHz was typically ~ 0.1 throughout the night, and the system temperatures ranged from 250 to 400 K depending on source elevation. Regular observations of MWC 349A were interspersed with those of KIC 8462852 for gain calibration. The quasar 3C273 was used for bandpass calibration, and Uranus was used for absolute flux calibration. We conservatively estimate a 20% uncertainty in the absolute flux calibration. Imaging was performed with natural weighting to maximize sensitivity, giving a synthesized beam of $4.4'' \times 2.8''$ at a position angle of 16.1° (measured east from north). We measure the 1σ continuum r.m.s. to be 0.73 mJy beam $^{-1}$.

2.3 Detected sub-mm sources in the SCUBA-2 image

We identified sources in the SCUBA-2 850 μm image by measuring the positions of peaks with greater than 4σ confidence in the map. A confidence level of 4σ corresponds to a false positive rate of $\sim 5\%$ (Roseboom et al. 2013; Chapin et al. 2013), which we considered to be a reasonable level for source detection. No $\geq 4\sigma$ sources were found in the 450 μm map which is fully consistent with our results at 850 μm given our 450 μm sensitivity and the typical spectral index of dust emission. The *Fellwalker* algorithm (Berry 2015) was used to locate the peaks. We list the detected sources, their coordinates and 850 μm fluxes in Table A1 (found in the online version of this paper). In total we detect 17 sources at 850 μm , with typical fluxes of a few mJy to 13.4 mJy.

We find no obvious positional matches between our catalogue and the Tycho-2 or UCAC4 stellar catalogues, which implies that the majority of 850 μm sources may be background sub-mm galaxies. The number counts of galaxies brighter than our 4σ detection threshold are indeed consistent with extragalactic number counts (10–20 galaxies brighter than this flux are predicted in an area the size of our daisy map; Coppin et al. 2006). However, given the relatively low Galactic latitude of our field ($b = +6.6$) we cannot rule out a Galactic origin for at least some of the sources. In particular, we find a significant association between TYC 3162-977-1 and *two* 850 μm sources which is discussed further in Sect. 4.

3 LIMITS ON THE AMOUNT OF DUST ASSOCIATED WITH KIC 8462852

We did not detect any significant emission toward KIC 8462852 in any of our observations, obtaining 3σ upper limits at the star’s position of 32.1, 2.55 and 2.19 mJy at 450, 850 and 1100 μm respectively. A 2.6σ peak is observed at the position of KIC 8462852 in the 850 μm SCUBA-2 image (see the closeup in Fig. 2) but we do not consider this to be a robust detection. We plot our upper limits plus the B15 and MHW15 photometry in Figure 3 together with three SED models discussed below.

At short wavelengths the observed emission is consistent with a purely photospheric origin from the star. At longer wavelengths *WISE*, SCUBA-2 and SMA provide only upper limits to any emission from circumstellar dust. This means that it is difficult to determine an absolute mass limit of any dust that may be associated with the star as we have few constraints on the underlying geometry (and hence temperature) of the dust distribution. However, the scenario-independent constraints proposed by B15 allow us to consider three hypothetical cases and determine the corresponding upper limits to their dust mass: *i*) where dust clumps are on circular orbits and are constrained by the dip durations to lie within 2 and 8 AU from the star; *ii*) where the dust clumps lie on highly elliptical orbits and the dip durations constrain them to lie within 0.1 and 26 AU; and *iii*) where the dust distribution is constrained to only be bound to the star with an outer radius of ~ 200 AU. We consider the bound of 200 AU to be an upper limit due to the presence of the companion to KIC 8462852.

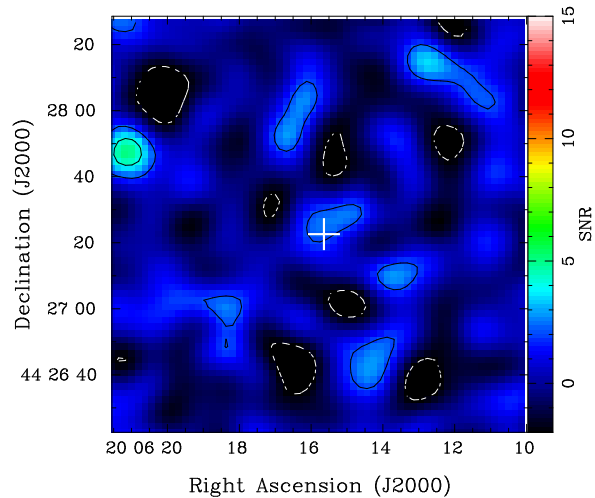


Figure 2. A close-up 850 μm signal to noise image of KIC 8462852, with the star indicated by a cross symbol. Contours are plotted at -2σ (white dashed contours), 2 and 4σ (black solid contours). KIC 8462852 is coincident with a 2.6σ peak in the image, but we do not consider this to be a robust detection.

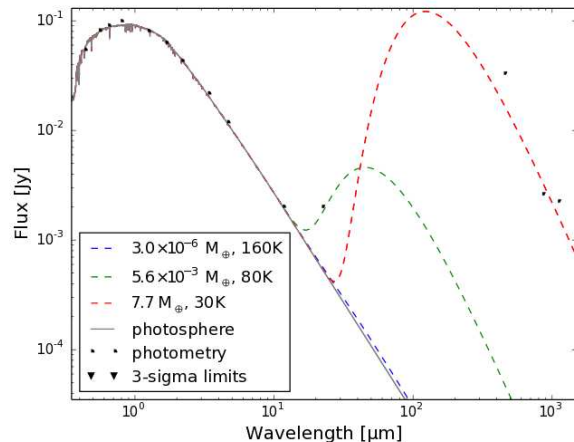


Figure 3. Spectral energy distribution of KIC 8462852 with archival photometry from B15 and MHW15 plus our SMA & SCUBA-2 upper limits. SED models corresponding to the scenarios discussed in Section 3 are also plotted.

To derive consistent upper limits on the mass of dust in the system, we compute grids of likelihoods for representative ranges of T_{dust} and M_{dust} consistent with each of our hypothetical cases, assuming that the stellar parameters are those given in B15 and that any dust emission takes the form of a modified blackbody. We assume a dust opacity κ_{ν} of $1.7 \text{ cm}^2 \text{ g}^{-1}$ at wavelength of 850 μm and a dust emissivity index $\beta = 1$ (e.g. Carpenter et al. 2005). As the dust emission is constrained only by upper limits on the excess flux, the likelihood for the model fluxes at these wavelengths becomes the probability that the model would be observed to have a flux below the 3σ limit, given the (rms-)uncertainty of the observation. By marginalising over the dust temperature, we derive upper limits to the dust mass by finding the minimum value that lies above at least 99.73% of the integrated likelihood.

For our three hypothetical cases we find upper limits to

the dust mass for case *i*) of $3.0 \times 10^{-6} M_{\oplus}$; for case *ii*) of $5.6 \times 10^{-3} M_{\oplus}$; and for case *iii*) of $7.7 M_{\oplus}$. The W3 and W4 upper limits place the tightest constraints on cases *i*) and *ii*), whereas the $850 \mu\text{m}$ upper limit constrains the total amount of cold dust present in the system.

Estimating an initial mass for colliding bodies that generate a particular amount of dust in a collision is not possible, given the wide range of variables in potential collisions. However an upper limit for dust within 8 AU of $\sim 10^{-6} M_{\oplus}$ makes the planetary collision hypothesis of B15 extremely unlikely. This amount of dust is comparable to a completely pulverised object of only a tenth of the mass of 1 Ceres. Of course, as MHW15 state, if the impactors were on an elliptical orbit the obscuring dust could have since moved to a more distant point where its now much cooler spectrum is below the *Spitzer* or *WISE* upper limits. Our SED models preclude this hypothesis by setting stringent limits of the order of a Pluto mass of dust out to at least 26 AU, which would require around 18 years for dust in a Keplerian orbit to travel this distance. Thus any planetary mass collision generating significant amounts of dust should have been detected in the MHW15 photometry.

B15's leading hypothesis, also favoured by MHW15 and Lisse, Sitko & Marengo (2015) is that the dimming events are caused by the breakup of a comet family. We can examine this hypothesis by inferring the minimum dust mass from that required to cause the obscuration in the *Kepler* light curve. We considered the quarter with the deepest absorption event (Q16) and computed the time-dependent optical depth from the light curve, converting optical depth to dust mass by assuming the same debris-disc like dust and stellar properties used to model the SED. By integrating over this mass and correcting for the crossing time as a function of assumed velocity we arrive at a lower limit to the mass of dust required to explain the obscuration.

For the orbits favoured by the dip duration, the resulting lower limit to the dust mass is of the order $10^{-9} M_{\oplus}$. This corresponds to a completely pulverised object with approximately 30 times the mass of Comet 1P/Halley. It is difficult to see how this dimming event could be caused by anything other than a truly remarkable family of comets. Our simple analysis agrees remarkably well with the more complex cometary modelling of Bodman & Quillen (2015) who estimate that the Q16 and Q17 dips require ~ 73 comets of radius 100 km (i.e. of the order of the radius of Comet C/1995 O1 Hale-Bopp).

The probability of observing a transit of a stellar radius clump of dust with a 0.1–1 AU periastron is 15–1.5%, which implies that either there is a mechanism to provide comets or comet clusters with similar orbital inclinations (perhaps the mean motion resonances discussed by Bodman & Quillen 2015), or that there is a much larger population of unseen non-transiting comets in the system. Our observations do not preclude the existence of a large Kuiper Belt or a large population of infalling comets on non-transiting orbits. However we note that there are no unusual absorption lines in the spectrum of KIC 8462852 presented by B15, which might be expected for a population of sun-grazing comets (e.g. Beust & Morbidelli 1996).

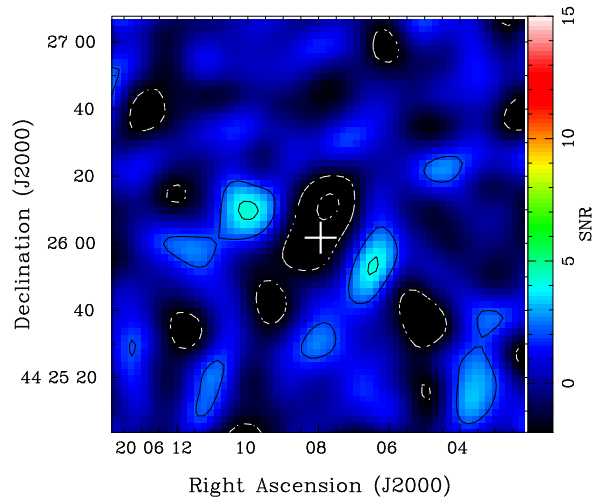


Figure 4. A close-up $850 \mu\text{m}$ signal to noise image of TYC 3162-977-1, with the star indicated by a cross symbol. Contours are plotted at -4 and -2σ (white dashed contours), 2 and 4σ (black solid contours). TYC 3162-977-1 is clearly seen in the negative bowl caused by the matched filtering process and is bracketed by two equidistant $\sim 4.3\sigma$ $850 \mu\text{m}$ sources.

4 TYC 3162-977-1: A POTENTIAL ~ 1000 AU EDGE ON DISC?

In Sect. 2.3 we did not find any stellar counterparts to single $850 \mu\text{m}$ sources. However the star TYC 3162-977-1 is equidistant from two ~ 4 mJy $850 \mu\text{m}$ sources (Fig. 4). The star appears to reside in a significant negative dip in the map, however this is an artefact caused by the matched filter applied in the data reduction (see Sect. 2.1). The overall morphology is reminiscent of the edge-on Fomalhaut system imaged with SCUBA by Holland et al. (2003) and so it is possible that we are seeing a similar disc-like structure around TYC 3162-977-1.

The close correspondence of star and $850 \mu\text{m}$ sources is unlikely to result from a chance alignment. We carried out a Monte Carlo simulation of the associations between a synthetic 1° radius Tycho-2 star catalogue corresponding to the Galactic latitude and longitude of the KIC 8462852 field and the SCUBA-2 Cosmology Legacy Survey UDS field (Geach et al. 2016, in prep). We found that there is only a 0.6% probability of finding a pair of $850 \mu\text{m}$ sources brighter than 4 mJy within $21''$ of a star in a region the size of our daisy map. We did not restrict our simulation to colinear alignments of star and sub-mm sources, nor to pairs of sources at similar flux, and thus we consider this probability to be a strict upper limit.

TYC 3162-977-1 is classified as a K7 V dwarf by Pickles & Depagne (2010) and a K4 V dwarf by Ammons et al. (2006), with estimated distances of 57 and 198 pc respectively. However, Pinsonneault et al. (2012) determine a $\log g$ value of 2.2, which is more consistent with a subgiant or giant star than a main sequence star. For a subgiant or giant star the $850 \mu\text{m}$ emission could be explained by a reheated debris disc or perhaps a detached stellar shell, whereas for a dwarf star the best explanation is an edge-on debris disc.

Regardless of the evolutionary state of TYC 3162-977-1, its distance, and the separation of the $850 \mu\text{m}$ sources im-

ply that - if it is a debris disc (reheated or not) - then its sub-mm extent (>1000 AU) is by far larger than that of *any* known such discs. The discs of β Pictoris and HR8799 (Larwood & Kalas 2001; Su et al. 2009) are seen to have a similar extent, but their extended emission results from small unbound dust grains blown away by radiation pressure. In contrast, at $850 \mu\text{m}$ we see larger, bound grains which are found to be in much smaller orbits in β Pictoris and HR8799 (Dent et al. 2014; Matthews et al. 2014). It is noteworthy that if β Pictoris were moved to a similar distance to TYC 3162-977-1 its $850 \mu\text{m}$ flux (Holland et al. 1998) would be ~ 4 mJy - similar to the fluxes we measure here.

5 SUMMARY AND CONCLUSIONS

We present 450, 850 and $1100 \mu\text{m}$ continuum observations of the peculiar star KIC 8462852 carried out with the Submillimeter Array and the SCUBA-2 camera on the James Clerk Maxwell Telescope. Our observations are the deepest photometry at these wavelengths yet obtained for this star, being roughly confusion limited at $850 \mu\text{m}$. We detected 17 sub-mm sources in the $850 \mu\text{m}$ image but no significant emission in the 450 & $1100 \mu\text{m}$ images. No significant emission is detected at the position of KIC 8462852 and we obtained 3σ upper limits at 450, 850, $1100 \mu\text{m}$ of 32.1, 2.55 and 2.19 mJy respectively. We draw the following conclusions:

(i) We determine upper limits to the dust mass for three hypothetical dust geometries in the KIC 8462852 system, corresponding to the “scenario-independent” constraints presented by B15. There is $\leq 3.0 \times 10^{-6} M_{\oplus}$ of dust lying 2–8 AU from the star; $\leq 5.6 \times 10^{-3} M_{\oplus}$ out to a radius of 26 AU; and an overall upper limit for dust within 200 AU of the star of $7.7 M_{\oplus}$. These limits make the catastrophic planetary collision hypothesis of B15 extremely unlikely.

(ii) From integrating the opacity in the *Kepler* lightcurve we obtain a lower limit to the amount of dust required to cause the deepest dip in the Q16 quarter of $\sim 10^{-9} M_{\oplus}$. This is consistent with more complex cometary models (Bodman & Quillen 2015) and requires a total amount of dust comparable to ~ 30 completely pulverised Comet Halleys. Our photometry limits do not rule out the existence of either a large population of infalling comets or the massive Kuiper Belt that would be their source.

(iii) We identify two $850 \mu\text{m}$ sources associated with the star TYC 3162-977-1 which are suggestive of an edge-on disc morphology. The probability of this being a chance association is $\leq 0.6\%$. The estimated distance to TYC 23162-977-1 implies that if this system is indeed a debris disc then it is by far the largest yet discovered with a ~ 1000 AU radius.

ACKNOWLEDGMENTS

The James Clerk Maxwell Telescope is operated by the East Asian Observatory on behalf of The National Astronomical Observatory of Japan, Academia Sinica Institute of Astronomy and Astrophysics, the Korea Astronomy and Space Science Institute, the National Astronomical Observatories of China and the Chinese Academy of Sciences (Grant No. XDB09000000), with additional funding

support from the Science and Technology Facilities Council of the United Kingdom and participating universities in the United Kingdom and Canada. This work is based partly on observations obtained with the Submillimeter Array, a joint project between the Smithsonian Astrophysical Observatory and the Academia Sinica Institute of Astronomy and Astrophysics and funded by the Smithsonian Institution and the Academia Sinica. MAT acknowledges support from the UK Science & Technology Facility Council via grant ST/M001008/1. FK acknowledges the support the Ministry of Science and Technology of Taiwan through grant MOST104-2628-M-001-004-MY3. JEG acknowledges the support of the Royal Society. MMD acknowledges support from the SMA through an SMA Postdoctoral Fellowship, and from NASA through grant NNX13AE54G.

REFERENCES

- Ammons S. M., Robinson S. E., Strader J., Laughlin G., Fischer D., Wolf A., 2006, *ApJ*, 638, 1004
 Arnold L. F. A., 2005, *ApJ*, 627, 534
 Berry D. S., 2015, *Astronomy and Computing*, 10, 22
 Beust H., Morbidelli A., 1996, *Icarus*, 120, 358
 Bodman E. H. L., Quillen A., 2015, *ArXiv e-prints*
 Boyajian T. S. et al., 2015, *ArXiv e-prints*
 Carpenter J. M., Wolf S., Schreyer K., Launhardt R., Hennig T., 2005, *AJ*, 129, 1049
 Chapin E. L., Berry D. S., Gibb A. G., Jenness T., Scott D., Tilanus R. P. J., Economou F., Holland W. S., 2013, *MNRAS*, 430, 2545
 Coppin K. et al., 2006, *MNRAS*, 372, 1621
 Dempsey J. T. et al., 2013, *MNRAS*, 430, 2534
 Dent W. R. F. et al., 2014, *Science*, 343, 1490
 Dyson F. J., 1960, *Science*, 131, 1667
 Forgan D. H., 2013, *Journal of the British Interplanetary Society*, 66, 144
 Harp G. R., Richards J., Shostak S., Tarter J. C., Vakoch D. A., Munson C., 2015, *ArXiv e-prints*
 Ho P. T. P., Moran J. M., Lo K. Y., 2004, *ApJ*, 616, L1
 Holland W. S. et al., 2013, *MNRAS*, 430, 2513
 —, 2003, *ApJ*, 582, 1141
 —, 1998, *Nature*, 392, 788
 Jenness T., Chapin E. L., Berry D. S., Gibb A. G., Tilanus R. P. J., Balfour J., Tilanus V., Currie M. J., 2013, SMURF: SubMillimeter User Reduction Facility. Astrophysics Source Code Library
 Larwood J. D., Kalas P. G., 2001, *MNRAS*, 323, 402
 Lisse C. M., Sitko M. L., Marengo M., 2015, *ArXiv e-prints*
 Marengo M., Hulsebus A., Willis S., 2015, *ApJ*, 814, L15
 Matthews B., Kennedy G., Sibthorpe B., Booth M., Wyatt M., Broekhoven-Fiene H., Macintosh B., Marois C., 2014, *ApJ*, 780, 97
 Pickles A., Depagne É., 2010, *PASP*, 122, 1437
 Pinsonneault M. H., An D., Molenda-Żakowicz J., Chaplin W. J., Metcalfe T. S., Bruntt H., 2012, *ApJS*, 199, 30
 Roseboom I. G. et al., 2013, *MNRAS*, 436, 430
 Stapledon O., 1937, *Star Maker*. Methuen
 Su K. Y. L. et al., 2009, *ApJ*, 705, 314
 Wright J. T., Cartier K. M. S., Zhao M., Jontof-Hutter D., Ford E. B., 2015, *ArXiv e-prints*

Table A1. Positions, fluxes and signal to noise ratios of sources detected in the 850 μm SCUBA-2 map.

Source ID	R.A. (J2000)	Dec. (J2000)	S ₈₅₀ (mJy)	SNR
SMM 1	20:05:53.3	+44:28:53	13.4	9.3
SMM 2	20:05:50.0	+44:27:26	11.3	6.8
SMM 3	20:06:30.0	+44:29:45	7.9	6.6
SMM 4	20:05:56.9	+44:28:45	8.1	6.0
SMM 5	20:06:28.7	+44:27:19	6.5	5.9
SMM 6	20:06:27.0	+44:31:25	7.7	5.6
SMM 7	20:05:56.5	+44:26:13	8.1	5.4
SMM 8	20:06:20.8	+44:27:47	4.6	5.0
SMM 9	20:06:38.0	+44:29:35	6.7	4.6
SMM 10	20:06:03.3	+44:24:15	6.7	4.5
SMM 11	20:05:59.7	+44:29:11	5.7	4.5
SMM 12	20:05:55.4	+44:29:39	6.1	4.5
SMM 13	20:06:15.2	+44:29:51	5.4	4.4
SMM 14	20:06:09.6	+44:26:09	4.6	4.3
SMM 15	20:06:06.1	+44:25:53	4.9	4.1
SMM 16	20:06:32.4	+44:24:37	5.4	4.0
SMM 17	20:06:24.7	+44:29:57	4.7	4.0

This paper has been typeset from a $\text{T}_{\text{E}}\text{X}/\text{L}^{\text{A}}\text{T}_{\text{E}}\text{X}$ file prepared by the author.

APPENDIX A: ONLINE MATERIAL